β^+ Gamow-Teller Strength in Nuclei

N. Auerbach [1], G. F. Bertsch, B. A. Brown, and L. Zhao

National Superconducting Cyclotron Laboratory and
Department of Physics and Astronomy
Michigan State University, E. Lansing, Ml 48824, USA

Abstract

The distribution of β^+ Gamow-Teller strength in ^{26}Mg, ^{54}Fe and ^{56}Ni is calculated. in the QRPA and large-basis shell-model spaces. The quenching relative to the simplest j j coupled model found in the QRPA is similar to that found in a shell-model basis which includes $2p-2h$ ground-state correlations within the major shell (sd or pf). For ^{26}Mg there is significant additional quenching found in the full sd shell-model space relative to the $2p-2h$ model space. We explore the connection between this additional quenching and the transition from jj to $SU(3)LS$ coupling via its relationship to the quadrupole collectivity. From this analysis we are able to estimate the total β^+ strength in ^{54}Fe and and ^{56}Ni which would be obtained in the full pf shell-model space. These calculations, together with the global quenching factor of 0.6, account for the observed strength in these nuclei. The quenching effects appearing in heavier nuclei are discussed.

[1] Permanent address: Tel-Aviv University, Tel-Aviv, Israel

1 Introduction

It is well known that the Gamow-Teller (GT) strength observed in low-lying (0-15 MeV) states in nuclei is about 40% less than that expected from the $S_- - S_+ = 3(N-Z)$ model-independent sum rule [1]. In many cases in heavy nuclei the total β^+ GT strength S_+ is expected to be very small compared to the β^- GT strength S_- and one can then deduce the quenching simply from the total S_- strength observed in (p,n) reactions [2]. In a few cases one has been able to deduce the quenching from a measurement of both the S_- and S_+ strength from (p,n) and (n,p) reactions, respectively [3, 4, 5]. However, the quenching deduced from the observation of only part of the GT spectrum (e.g. from the β^+ spectrum alone or only from the beta decay to selected low-lying states) is model dependent.

In this work we address the question of the relatively large quenching observed for the S_+ strength (in nuclei with $N > Z$) relative to the single-particle jj coupled shell-model estimate, in particular for ^{26}Mg, ^{54}Fe and ^{56}Ni. We explore the interrelationships between various approximations for the model spaces beyond the jj coupling limit, some aspects for the first time. The role of $2p-2h$ ground-state correlations within a major shell (i.e. the sd shell or pf shell) is reexamined. We find that the QRPA and $2p-2h$ shell-model calculations (carried out with the same residual interaction) give essentially the same result for the total S_+ strength, whereas the splitting and fine-structure of the strength is realistic only in the shell-model calculation. We also consider correlations beyond $2p-2h$ by calculating the strength for the case of ^{26}Mg in the sd shell where the full major-shell basis can be included. For this sd case we find about a factor of two additional quenching relative to the $2p-2h$ model space. The implication of this additional quenching is explored with regard to the transition between jj and $SU(3)LS$ coupling and the associated quadrupole collectivity which can be observed in the the low-lying 0^+ to 2^+ B(E2) values. We find that ^{26}Mg is close to the $SU(3)$ limit whereas ^{54}Fe and ^{56}Ni are closer to the jj limit. Our final values for the total S_+ strength (which includes in addition the global quenching factor of 0.6 due in part to the $2p-2h$ correlations outside of the major shell) are in good agreement with experiment for ^{26}Mg and ^{54}Fe. The very small GT matrix element obtained from the $2p-2h$ shell-model calculation for the beta decay of ^{56}Ni to the 1.72 MeV state in ^{56}Co is in qualitative agreement with experiment. Implications of these results for other cases will be discussed.

The sum rule is given by

$$S_- - S_+ = \sum_f < f|\mathrm{GT}_-|i >^2 - \sum_f < f|\mathrm{GT}_+|i >^2 = 3(N-Z), \qquad (1)$$

with

$$\mathrm{GT}_\pm = \sum_k \sigma(k) t_\pm(k), \qquad (2)$$

where f and i label the initial and final states, respectively, and the summation is over all of the nucleons. N and Z are the proton and neutron numbers in the initial state nucleus. Two mechanisms have been proposed in order to explain the missing GT strength relative to this sum rule. In one of them the interaction of the GT resonance with a Δ-particle nucleon-hole state is responsible for removing the strength to very high excitation energies (about 300 MeV) [1]. In the second approach the GT strength is spread out, due to the action of a residual nuclear force, into many $2p-2h$ configurations lying at excitation energies of $10 \sim 50$ MeV above the main GT peak [6]. The combined contribution of both mechanisms may very well be the answer to the problem of the missing GT strength.

How important are the nuclear correlations within the same major shell as far as the question of missing GT strength is concerned ? Not very much if the quenching is discussed only in the context of the $3(N-Z)$ sum rule. Eq. 1 assures that if the ground state correlations will affect the S_- strength they will affect also the S_+ in the same manner so as to cancel in the above sum rule. Thus, the question of the ground state correlations is directly connected to the S_+ (β^+-GT) strength [7].

In a number of nuclei GT_+ transitions are not blocked and one observes that β^+-decay transitions are strongly quenched as compared with estimates provided by the jj single-particle model. The quenching factors range between $2 \sim 30$ [8]. Since the experimental data concerning the GT_+ strength in the $A = 100 \sim 160$ region comes only from the actual β^+ decays it is limited only to the range of energies accessible by these decays.

In a number of cases [8], it is clear, however, that the total GT_+ strength is indeed very strongly quenched. Several models were suggested in order to explain the large quenching factors [9, 10]. The observation of an entire GT_+ strength distribution in (n,p) reactions together with the distribution GT_- obtained in (p,n) experiments is extremely useful in separating the various sources of quenching.

2 The (n,p) reaction and GT_+ strength

The (n,p) charge-exchange reaction is one of the best and efficient ways of trying to map out the GT_+ strength in nuclei. The experience and understanding gained in studying the (p,n) reaction mechanisms is immediately applicable to the (n,p) reaction. Several (n,p) experiments were performed in the recent years at TRIUMF and LAMPF. One very detailed study of the $^{54}Fe(n,p)^{54}Mn$ was performed in the last few years [3] and has been the basis of RPA theoretical studies [11, 12]. This data together with the existing (p,n) data should provide a testing ground for the various approximation schemes [10, 13, 14] (RPA, QRPA, etc) used recently in describing charge exchange and the nuclear structure aspects of the double beta decay process. In addition, we consider the GT_+ strength in ^{26}Mg for which experimental data is also available [4, 5].

For the ^{54}Fe target, the GT_+ transitions are allowed in the limit of a pure shell-model configurations. An initial of $(\pi j_>^{n_\pi})(\nu j_>^{2j_>+1})$ configuration leads to [12]:

$$S_+ = n_\pi \frac{4l}{2l+1} = \frac{72}{7}, \tag{3}$$

as compared to

$$S_- = (2j_> + 1)\frac{4l}{2l+1} + (2j_> + 1 - n_\pi)\frac{2l+3}{2l+1} = \frac{114}{7}. \tag{4}$$

where the numerical results in this case are obtained for $j_> = f_{7/2}$, $2j_> + 1 = 8$, and $n_\pi = 6$. The S_+ is simply related to the $(\pi f_{7/2}) \rightarrow (\nu f_{5/2})$ transition of each of the six $f_{7/2}$ protons (π) into a $f_{5/2}$ neutron (ν). The first term in the S_- expression is for the $(\nu f_{7/2}) \rightarrow (\pi f_{5/2})$ transitions and the second term is for the $(\nu f_{7/2}) \rightarrow (\pi f_{7/2})$ transitions.

The experimental results for these two strengths as measured in the (n,p) and (p,n) experiment [3, 14] are

$$S_+ = 3.1 \pm 0.6 \text{ and } S_- = 7.8 \pm 1.9.$$

Considering the ^{56}Ni to be a closed core nucleus the GT_+ strength consists of transitions in which each of the eight protons in the $f^8_{7/2}$ configuration is transformed into an $f_{5/2}$ neutron. The GT strength for such type of transition is obtained from Eq. 4 with $n_\pi = (2j_> + 1) = 8$ which gives $S_- = S_+ = 13.7$.

3 Calculation of GT_+ strength

In a paper [12] based on a previous work [11] the quenching by factor of more than two of S_+ in ^{54}Fe was explained by involving the charge-exchange

RPA scheme. It was argued that about 30 % of the quenching of the S_+ strength is due to the universal quenching mechanism [1, 2] (also present in the S_- strength) but that the main reduction of GT_+ strength (additional 50 %) comes from RPA correlations in the ground state. (In the work of ref. 10, the RPA quenching factor for ^{54}Fe was assumed to be the same as calculated earlier for ^{60}Ni [11].) The ground state correlations resulting from this charge-exchange RPA come into play because in the case of ^{54}Fe both GT_+ and GT_- transitions are not Pauli blocked and the particle-hole (ph) configurations of GT_- type make up the "backward going" graphs for the GT_+ transitions and vice versa, the GT_+ ph configurations are the "backward going" graphs for the GT_-.

In spite of the nice agreement with the recent experiments the question still remains how accurate is such a charge-exchange RPA calculation, in this case ? How would other shell-model type correlations affect the GT_+ strength in the ^{54}Fe case ? The aim of this work is to examine this question.

We have therefore computed the distribution of GT strength in ^{54}Fe and ^{56}Ni in an extended shell-model space. For comparison also small space shell-model calculation were performed. The computations were done using the shell-model code OXBASH [15]. In order to examine the sensitivity of the results to the truncation of the shell-model space we have performed analogous calculations also for the ^{26}Mg $\rightarrow$ ^{26}Na GT_+ transitions. In this case, however, it was possible to perform a completely unrestricted shell-model calculation within the sd shell.

For the pf shell we use the MSOBEP [16] interaction with the single-particle energies adjusted to reproduce the lowest (single-particle) states in ^{55}Ni and ^{57}Ni under the assumption of a closed-shell configuration for these states. For the sd shell we use the Brown-Wildenthal USD [17] interaction. The RPA and QRPA calculations discussed below were carried out with the USD and MSOBEP interactions for both the RPA and BCS components of the calculations. The BCS was carried out exactly with state-dependent pairing gaps. In addition the RPA and QRPA include explicitly the rearrangement terms for the single-particle energies (such rearrangement terms are included implicitly in the shell-model calculations.)

We have performed the following types of calculations:

(a) the simplest calculation consists of β^+ type GT transitions from the pure $f_{7/2}^n$ configuration ($n = 14$ for ^{54}Fe and $n = 16$ for ^{56}Ni) to the pure $f_{7/2}^{n-1} f_{5/2}$ configuration, and $d_{5/2}^{10}$ to the $d_{5/2}^{10} d_{3/2}$ in the $^{26}\mathrm{Mg} \rightarrow {}^{26}\mathrm{Na}$ GT$_+$ case.

(b) In the next, more complex calculation we include configuration mixing between the $f_{7/2}^n$ and $f_{7/2}^{n-2} f_{5/2}^2$ configurations. In the $A = 56$ case, we, therefore, have in the ground state of ^{56}Ni for the protons the mixed $0p - 0h$ and $2p - 2h$ configurations of the type, $a f_{7/2}^8 + b f_{7/2}^6 f_{5/2}^2$. The GT$_+$ transition occurs between such admixed state and between the $J^\pi = 1^+$ states of $1p - 1h$, $2p - 2h$ and $3p - 3h$ configurations formed from the $f_{7/2}$ and $f_{5/2}$ orbits. The results are shown in Table 1 and labeled as the SM $2p - 2h$(r) calculations, where "r" indicates that the model space is restricted to two orbitals $j_>$ and $j_>$. Similar calculations were performed for ^{26}Mg and ^{54}Fe and are also shown in Table 1.

(c) How does the quenching change when more orbitals are employed in the calculation? We performed calculation in which in the initial state up to two particles are promoted from the $f_{7/2}$ or $d_{5/2}$ single-particle state into $(p_{3/2}, f_{5/2}, p_{1/2})$ or $(s_{1/2}, d_{3/2})$ single-particles states, and in the final states up to three particles are promoted from the pure configuration. We will label these calculations as the SM $2p-2h$.

(d) For ^{56}Ni, we have carried out the charge-exchange RPA calculations which involve neutron-particle proton-hole excitations. The ^{56}Ni nucleus was treated as a closed shell and of course the RPA introduces in the ground state $2p-2h$ correlations of specific nature. The results are shown in Table 1 and Fig. 3. In the ^{54}Fe and ^{26}Mg nuclei, the neutron shell is open. In order to include the effect of pairing correlations among the valence neutrons one adopts the quasi particle scheme by transforming particles into quasi-particles using the Bogoliubov-Valatin transformation. The transformed (BCS) ground state is then used as the basis for the RPA. Such a scheme is termed the QRPA and was used in recent years to study excitations of medium and heavy mass nuclei with open shells [10, 18]. When one allows for the QRPA excitations to involve charge-exchange transitions, one obtains the scheme termed pnQRPA. This scheme was applied extensively to the study of double-beta decay transitions in nuclei [18]. (In this context it was also applied to the ^{54}Fe nucleus [19].) Our RPA and QRPA calculations were carried out with the same input for the residual interactions and single-particle energies that went into the more complete shell-model calculations The results of our pn-QRPA calculations for ^{26}Mg and ^{54}Fe are shown in Table 1 and depicted in Fig.1. and Fig.2, respectively.

(e) Finally for the ^{26}Mg $\rightarrow$ ^{26}Na transition is was possible to perform a full shell-model calculation in which all possible configurations in the *sd* shell are included. The results are shown in Table 1 and Fig. 1.

4 Discussion of the results and conclusion

For the pure $f_{7/2}$ configuration, the total GT$_+$ strength (S_+ = 13.71) in the ^{56}Ni $\rightarrow ^{56}$Co transition is contained in one state located at an excitations energy of E_x = 10.3 MeV. In the ^{54}Fe $\rightarrow ^{54}$Mn case, the strength of S_+ = 10.29 is distributed among a few states centered around the excitation energy of about 10 MeV. Also in the ^{26}Mg $\rightarrow$ ^{26}Na case the S$_+$ strength (S$_+$=6.4) is contained in a few states located between 11-15 MeV.

As one expands the shell-model space to include $2p-2h$ configurations, the total S_+ strength is reduced significantly from the pure configuration case. In the SM $2p-2h$ calculation a substantial reduction of strength occurs. The total S_+ strength in the ^{56}Ni $\rightarrow ^{56}$Co transition is about 10.38 which is a 25 % reduction in the strength. In the ^{54}Fe $\rightarrow ^{54}$Mn case the strength in the SM

$2p-2h$ calculation is 7.05. This constitutes a 32 % reduction in strength. The reduction of strength in the $^{26}Mg \to {}^{26}Na$ in this type of calculation is 42 %. The SM $2p-2h$ calculations are very similar to the the more restricted $2p-2h$(r) calculations.

How do these results of the extended shell model compare with the RPA and QRPA ? In ^{56}Ni, the quenching factor obtained in the RPA is very close to the one obtained in the SM $2p-2h$ calculations. The same holds also in the case of ^{54}Fe where the extended shell model is compared to the QRPA. Again the quenching factors in the pnQRPA and SM are in agreement. In the ^{26}Mg case QRPA gives a quenching factor of 56 %, somewhat larger than the quenching factor obtained in the $2p-2h$. (Another recent comparison of SM and QRPA for A=26 was made with the same methods and the interaction used here'[20], however, the results differ from ours for reasons which are not understood.) We may therefore argue, in accordance with the conjecture made in refs [12], that a substantial contribution to the quenching of GT_+ strength comes from RPA type correlations in the ground states.

Our extended shell-model calculations for ^{54}Fe and ^{56}Ni are carried out in a space that contains up to $2p-2h$ configurations, and not the full pf shell space. What would be the effect of an enlarged configuration space beyond $2p-2h$ states? It is practically impossible, at the present, to provide a direct answer by performing a full calculation in the pf shell. One can however get some guidance from a the full shell-model calculation of the GT transition

^{26}Mg $\rightarrow^{26}$Na. In Fig. 1, we show the calculated GT$_+$ strength for $A = 26$ case for various stages of shell-model approximations and for the pnQRPA. We note that in the full SM model space, an additional (almost a factor of two) quenching of GT$_+$ strength occurs relative to the $2p - 2h$ calculation.

We may use the *sd* shell results as guidance for the *pf* shell by considering its relationship to the transition between *jj* to $SU(3)LS$ coupling and the associated change in quadrupole collectivity. In the $SU(3)LS$ limit the GT$_+$ strength is zero [since all of the GT strength resides in a single GT$_-$ transition which exhausts the $3(N - Z)$ sum rule] and the quadrupole collectivity [the B(E2) value connecting the ground state and first 2^+ state in ^{26}Mg] is at or near its maximum possible value. This relationship is illustrated in Fig. 4 where the ratio of S_+ to the $0p - 0h$ SM estimate, R_+, is plotted vs the B(E2,$2^+ \rightarrow 0^+$) value. The points (circles) in Fig. 4 correspond to the $0p - 0h$, $2p - 2h$, full and $SU(3)$-limit values as a function of increasing B(E2) [decreasing R_+]. There is seen to be a simple monotonic relationship between R_+ and B(E2) which is about linear between the $2p - 2h$ and $SU(3)$-limit values. The B(E2) in the $SU(3)$ limit was obtained by using an $SU(3)$ conserving Hamiltonian [21] for the full-basis SM calculations and is in agreement with the value obtained from the analytical formulae [22]. The experimental B(E2) value for ^{26}Mg [23] is in good agreement with the full *sd* SM (USD-interaction) value.

Our calculated B(E2) values incorporate effective charges of 1.35 *e* and

0.35 e for the proton and neutron, respectively, which take into account the coupling to the $2\hbar\omega$ excitations. For the sd shell nuclei it has been shown empirically that the degree of collectivity is governed by the $0\hbar\omega$ sd shell wave functions and that the contribution of the $2\hbar\omega$ is predominantly in terms of an overall (nucleus and state independent) renormalization which is accounted for in terms of the effective charge [17]. Thus, both the E2 and GT properties are mainly determined by the $0\hbar\omega$ structure.

We can now add to Fig. 4 the $2p-2h$ and $SU(3)$-limit values for ^{54}Fe (squares). The experimental B(E2) for ^{54}Fe [23] falls at the point indicated by the cross in Fig. 4, where we have arbitrarily chosen a reasonable interpolated value value of R_{+}=0.62 for this point. The S_{+} values resulting from this interpolation are given in the column headed "SM full" in Table 1 [we assume the same R_{+} value for ^{56}Ni].

The type of quenching discussed up to this point is only due to correlations with the valence major-oscillator shell (sd or pf) and has little affect the $3(N-Z)$ sum rule for the low-lying states. In order to be able to compare to experiment one must take into account the more universal quenching that affects the $3(N-Z)$ sum rule for low-lying states. This can be done by introducing an effective GT transition operator

$$\tilde{\sigma} t = c \sigma t \tag{5}$$

where c is a renormalization constant. Experiments tell us that the $3(N-Z)$ sum rule is quenched by 40 %. Thus all the transition strengths have to be reduced by a factor of $c^2 = 0.6$ ($g_A(\text{eff}) = \sqrt{0.6}\ g_A$.) These numbers for the full shell-model case are shown under the column labeled "full SM(eff)" of Table 1. For the $^{54}Fe \rightarrow ^{54}Mn$ and $^{26}Mg \rightarrow ^{26}Na$ transitions, the S_+ strengths obtained in the extended shell model are in the range of experimental values given in the last column of Table 1.

Our empirical relation between the S_+ GT strength and the B(E2) appears to be supported by recent experimental data [25] which shows about a 35 % reduction in the S_+ strength in ^{56}Fe compared to ^{54}Fe, whereas the product of the S_+ strength and the B(E2) value is nearly constant. (Shell-model calculations of the $2p-2h$ type predict about the same S_+ strength for both nuclei [9].)

We should mention here a few other points when trying to compare results with experiment. In Fig. 2 we show the GT_+ strength in the $A = 54$ case as measured in ref. [3]. The shape of the distribution is in agreement with the SM $2p-2h$ calculation. (Note that the calculated strengths in Fig. 2 do not contain the universal quenching factor of 0.6). The β^+ decay of ^{56}Ni to ^{56}Co was recently remeasured [24]. The decay to the lowest 1^+ state in ^{56}Co (at E_x=1.72 MeV) was observed with a logft of 4.4 which gives $B(GT_+) = \langle f|GT_+|i\rangle^2 = 0.16$. This should be compared with the value of $B(GT_+)=0.38$ obtained in our calculation for the lowest 1^+ state in the SM $2p-2h$(eff) calculation. The agreement is reasonable in the sense that the lowest B(GT) value to the 1^+ state is very small compared to the total strength in both experiment and theory. We note that the transition with the largest B(GT) value in this case is predicted to be to a state 0.65 MeV higher in energy which is outside of the Q-value window for this decay.

In heavier nuclei the quenching of GT_+ strength as already mentioned, is much larger, reducing the strength sometimes by factors of ten or more. In several previous studies [9, 10], it was pointed out that the large quenching factors in β^+ transitions in heavy mass nuclei ($A > 100$) are a result of particular kinds of proton-neutron correlations which do not exist in the simple RPA scheme but do appear when a BCS wave function is used as a vacuum in the QRPA calculation.

In the shell-model language the correlations introduced by the QRPA can be visualized in the following simple example. Let us take a single orbit configuration, say $(\pi j_>^{n_\pi})(\nu j_>^{n_\nu})$ to be the vacuum state. In the Tamm-Dancoff approximation (TDA), the GT_+ strength is due, for example, to transitions to $(\pi j_>^{n_\pi-1})(\nu j_>^{n_\nu+1})(1^+)$ or $(\pi j_>^{n_\pi-1})(\nu j_<)(\nu j_>^{n_\nu})(1^+)$ transitions. The use of the RPA consists of introducing in the ground state $2p-2h$ admixtures of the type $\{(\pi j_<)(\nu j_>^{n_\nu-1})(1^+);(\pi j_>^{n_\pi-1})(\nu j_<)(1^+)\}(0^+)$. These are induced by the residual proton-neutron ph, $V_{\sigma\tau}$ force. These $2p-2h$ components in the RPA ground state allow for additional contributions to $GT_\pm$ transitions. These are of the type $(\nu j_<) \rightarrow (\pi j_>)$ for GT_- and $(\pi j_<) \rightarrow (\nu j_>)$ for GT_+. These contributions to the strength are referred as the "backward" going graphs (the Y amplitudes). The Y-amplitudes, for a repulsive ph interaction, lead to a reduction of $GT_\pm$ strength. This is the situation before pairing is introduced.

A strong pairing force will produce ground state configurations in which a $J^\pi = 0^+$ pair of identical nucleons (protons or neutrons) is excited into a higher orbit, in our example from the $j_>$ into the $j_<$ orbit. The ground state will consist of configurations:

$$\alpha(\nu j_>^{n_\nu})(0^+) + \beta(\nu j_>^{n_\nu - 2})(\nu j_<^2)(0^+), \tag{6}$$

and similarly for protons (π).

With such pairing ground state as the basis one may apply the RPA. In addition to the usual $2p - 2h$ correlations introduced by the residual ph force and the corresponding Y amplitudes one will also have a residual particle-particle, proton-neutron interaction which will lead to new admixtures in the QRPA ground states. The new components will have the form $(\pi j_>^{n_\pi - 1})(\pi j_<)(\nu j_>^{n_\nu - 1})(\nu j_<)$. The size of this admixture will be proportional to the pairing occupation parameter β of orbit $j_<$. The $GT_\pm$ operator is now able to connect this component in the ground state to the final GT_+ or GT_- configurations, giving rise to a new $GT_\pm$ amplitude. For an attractive particle-particle interaction, the contribution of this amplitude to the GT_- and GT_+ strength is such that it leads to additional quenching of strength.

The above consideration serves only as a simple illustration of the physics involved in the pnQRPA. In practice there are many more orbits that contribute and initial ground state has a rather complicated structure, best described by a BCS wave function. The results of the various QRPA calculations indicate that the quenching in the GT_+ strength in heavy mass nuclei, due to the correlations induced by the particle-particle (V_{pp}) interaction, could be very large almost a factor of two [10]. In a nucleus such as ^{148}Dy the quenching factors stemming from the QRPA are of the order four to five. For some values of V_{pp} the quenching might even be larger [10]. We would like to contrast this factor with the results we obtained here for $A = 26$, $A = 54$ and $A = 56$ nuclei. We have seen that in the extended shell-model calculation (which certainly incorporates the kind of correlations found in QRPA) the quenching factor for GT_+ in ^{54}Fe and ^{56}Ni is only about two. This, as already mentioned, is very close to the quenching found in the QRPA or RPA for these nuclei. To reconcile this result with the large quenching factor found in QRPA computations in heavier nuclei one must conclude that pairing effects are not as important in lighter nuclei as they are in the heavier ones.

5 Acknowledgments

Research Supported in part by the National Science Foundation under Grant No. PHY-90-17077.

6 Figure captions

Fig. 1: Running sum of the $B(GT_+)$ values for ^{26}Mg vs. excitation energy. S_+ is the total value at Ex=25 MeV. The labels correspond to the headings in Table 1.

Fig. 2: Running sum of the $B(GT_+)$ values for ^{54}Fe vs. excitation energy. S_+ is the total value at Ex=25 MeV. The labels correspond to the headings in Table 1.

Fig. 3: Running sum of the $B(GT_+)$ values for ^{56}Ni vs. excitation energy. S_+ is the total value at Ex=25 MeV. The labels correspond to the headings in Table 1.

Fig. 4: R_+ vs B(E2) for the $0p-0h$, $2p-2h$, full and $SU(3)$-limit calculations for ^{26}Mg (filled circles), and the $0p-0h$, $2p-2h$ and $SU(3)$-limit calculations for ^{54}Fe (squares). The cross corresponds to the experimental B(E2) value for ^{54}Fe. See text for details.

Table 1: Calculated S_+ values

^{A}Z	SM $0p-0h$	SM $2p-2h(r)$ (a)	SM $2p-2h$ (b)	RPA or QRPA	SM full	SM full(eff) (c)	Exp
^{26}Mg	6.4	3.38	3.72	2.84	1.72	1.03	1.3±0.6 (e), 0.84(f)
^{54}Fe	10.29	6.68	7.05	6.70	6.4(d)	3.8(d)	3.1±0.6(g)
^{56}Ni	13.71	9.81	10.38	10.27	8.5(d)	5.1(d)	

a) $(d_{5/2}, d_{3/2})$ model space for ^{26}Mg and $(f_{7/2}, f_{5/2})$ model space for ^{54}Fe and ^{56}Ni.

b) $(d_{5/2}, d_{3/2}, s_{1/2})$ model space for ^{26}Mg and $(f_{7/2}, f_{5/2}, p_{3/2}, p_{1/2})$ model space for ^{54}Fe and ^{56}Ni.

c) $g_A(\text{eff}) = \sqrt{0.6}\ g_A$.

d) Estimates based on the ^{26}Mg calculation (see text).

e) From the (p,n) data of Ref. [4]. As discussed in this reference, the lower bound follows from assuming only the 13.6 MeV state has T=2 and the upper bound from assuming that all 1^+ states between 13.6 and 15 MeV in excitation are T=2.

f) From the (n,p) data of Ref. [5].

g) From the (n,p) data of Ref. [3].

References

[1] M. Ericson, A. Figereau, and D. Thevenet, Phys. Lett. **45B** (1973), 19; E. Oset and M. Rho, Phys. Lett. **42** (1979), 47; I. Towner and F.C. Khana, *ibib* **42** (1979), 51; G. Bertsch, Nucl. Phys. **A354** (1981), 157; A. Bohr and B.R. Mottelson, Phys. Lett. **100B** (1981), 10; G.E. Brown and M. Rho, Nucl. Phys. **A372** (1981), 397; B. A. Brown and B. H. Wildenthal, At. Data Nucl. Data Tables **33** (1985), 347.

[2] C.D. Goodman, et.al Phys. Rev. Lett. **44** (1980), 1755; C. Gaarde, et.al, Nucl. Phys. **A334** (1980), 248; C. D. Goodman, Can. Jour. Phys. **65** (1990), 574.

[3] M.C. Vetterli, et.al, Phys. Rev. Lett. **59** (1987), 439; M.C. Vetterli, et.al, Phys. Rev. **C40** (1989), 559.

[4] R.Madey et al., Phys. Rev. **C35** (1987), 2011; **C36** (1987), 1647.

[5] S. Yen, Can. Jour. Phys. **65** (1987), 595.

[6] G.F. Bertsch and I. Hamamoto Phys. Rev. C **26** (1982), 1323; D. Cha and J. Speth, Phys. Rev. **C31** (1985), 372; A. Klein, W.G. Love and N. Auerbach, Phys. Rev. **C31** (1985), 710.

[7] N. Auerbach, A. Klein and W.G. Love, in Proceedings of the conference on "Antinucleon and Nucleon Nucleus Interaction", Ed. G.E.

Walker, C.D. Goodman and C. Olmer, plenum publishing corporation, 1985, p323.

[8] A.H. Wapstra and N.B. Gove, Nucl. Data Table **9** (1971), 265; Kleinheinz, et. al., Phys. Rev. Lett. **55** (1985), 2664.

[9] I.S. Towner, Nucl. Phys. **A444** (1985), 402; S.D. Bloom and G.M. Fuller, Nucl. Phys. **A440** (1985), 511.

[10] D. Cha, Phys. Rev.**C27** (1983), 2269.

[11] N. Auerbach, L. Zamick and A. Klein, Phys. Lett **118B** (1982), 256.

[12] N. Auerbach, Phys. Rev. **C36** (1987), 2694.

[13] G. Bertsch and H. Esbensen, Reports on Progress in Physics, **50** (1987), 607.

[14] J. Rappaport, et. al. Nucl. Phys. **A427** (1984), 332

[15] A. Etchegoyen, W.D.M. Rae, N.S. Godwin, W.A. Richter, C.H. Zimmerman, B.A. Brown, W.E. Ormand and J.S. Winfield, MSU-NSCL report #524 (1985).

[16] W.A. Richter, M.G. Van der Merwe, R.E. Julies and B.A. Brown, Nucl. Phys. **A523** (1991), 325.

[17] B. A. Brown and B. H. Wildenthal, Ann. Rev. Nucl. Part. Phys. **38** (1988), 29 and references therin.

[18] K. Grotz and H.V. Klapdor, Nucl. Phys. **A460** (1986), 395; P. Vogel and M.R. Zirnbaur, Phys. Rev. Lett., **57** (1986), 3148; O. Civitarese, A. Faessler and T. Tomoda, Phys. Lett. **194B** (1987), 11.

[19] J. Engel, P. Vogel and M.R. Zirnbauer, Phys. Rev. **C37** (1988), 731.

[20] O. Civitarese et al., J. Phys. G **17** (1991), 1363.

[21] M. Harvey, Adv. Nucl. Phys. **1** (1968) 67.

[22] J. P. Elliott, Proc. Roy. Soc. (London), **A245** (1958), 128 and 562.

[23] P. M. Endt, At. Data and Nucl. Data Tables **23** (1979), 3 adn 547.

[24] B. Sur et al., Phys. Rev. **C42** (1990), 573.

[25] T. Ronnqvist et al., preprint 1993.

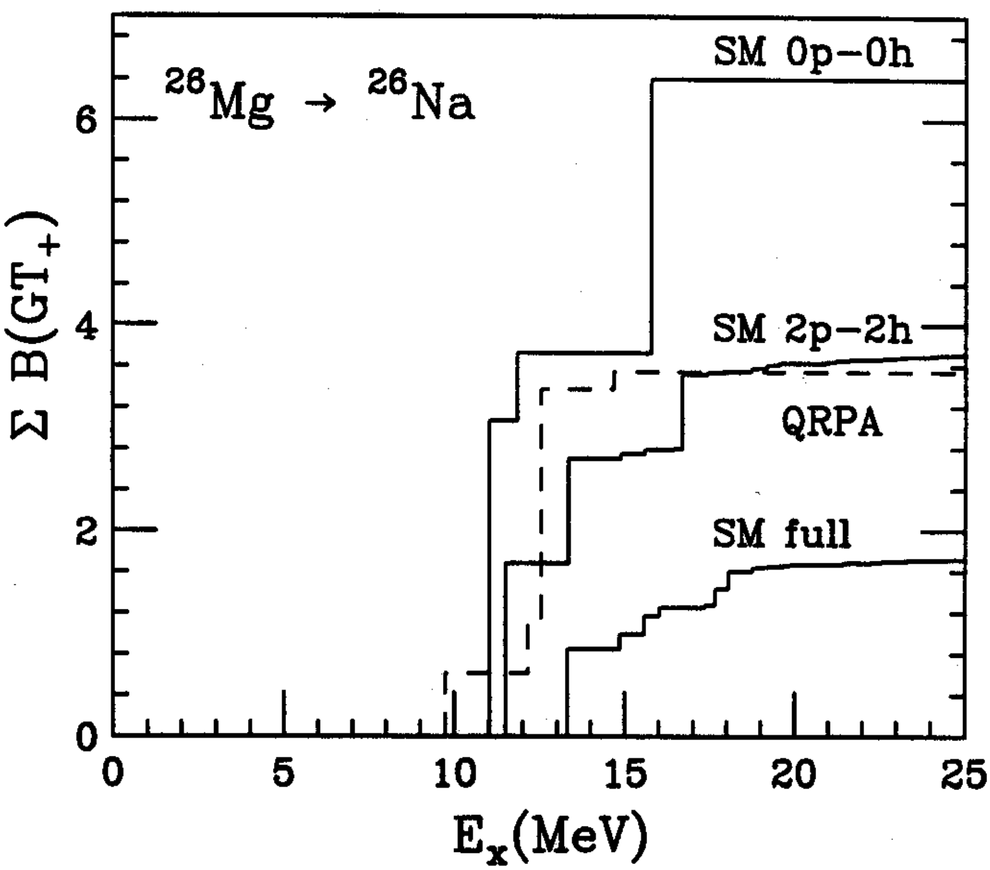

$^{26}Mg \rightarrow {}^{26}Na$
SM 0p−0h
SM 2p−2h
QRPA
SM full
0
2
4
6
0
5
10
15
20
25
Σ B(GT+)
Ex(MeV)

Fig. 1

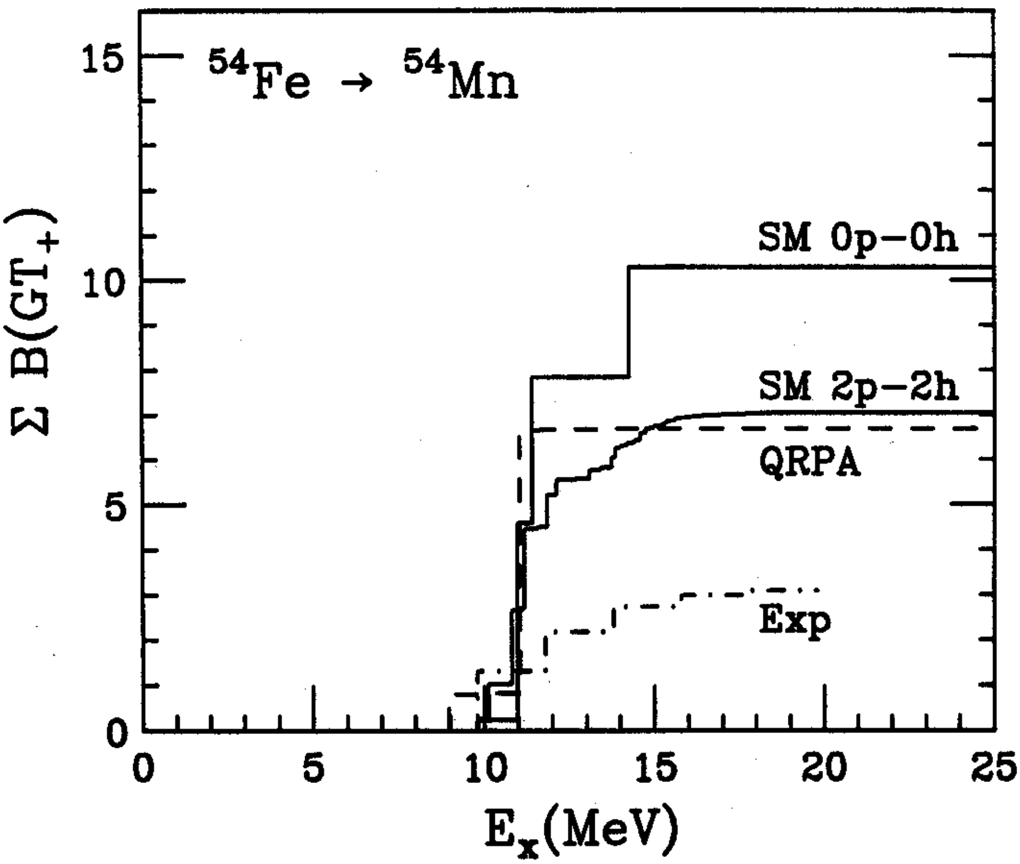

Fig. 2

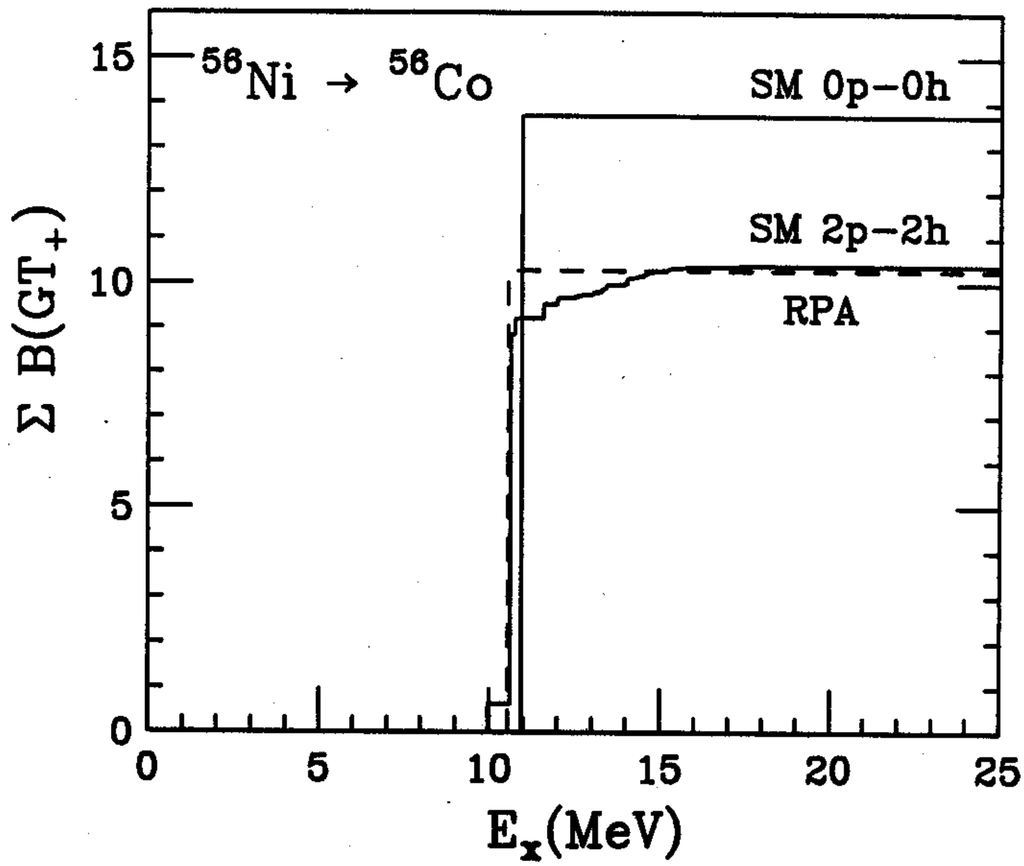

$^{56}Ni \rightarrow {}^{56}Co$
SM 0p−0h
SM 2p−2h
RPA
Σ B(GT$_+$)
E_x(MeV)
0
5
10
15
20
25

Fig. 3

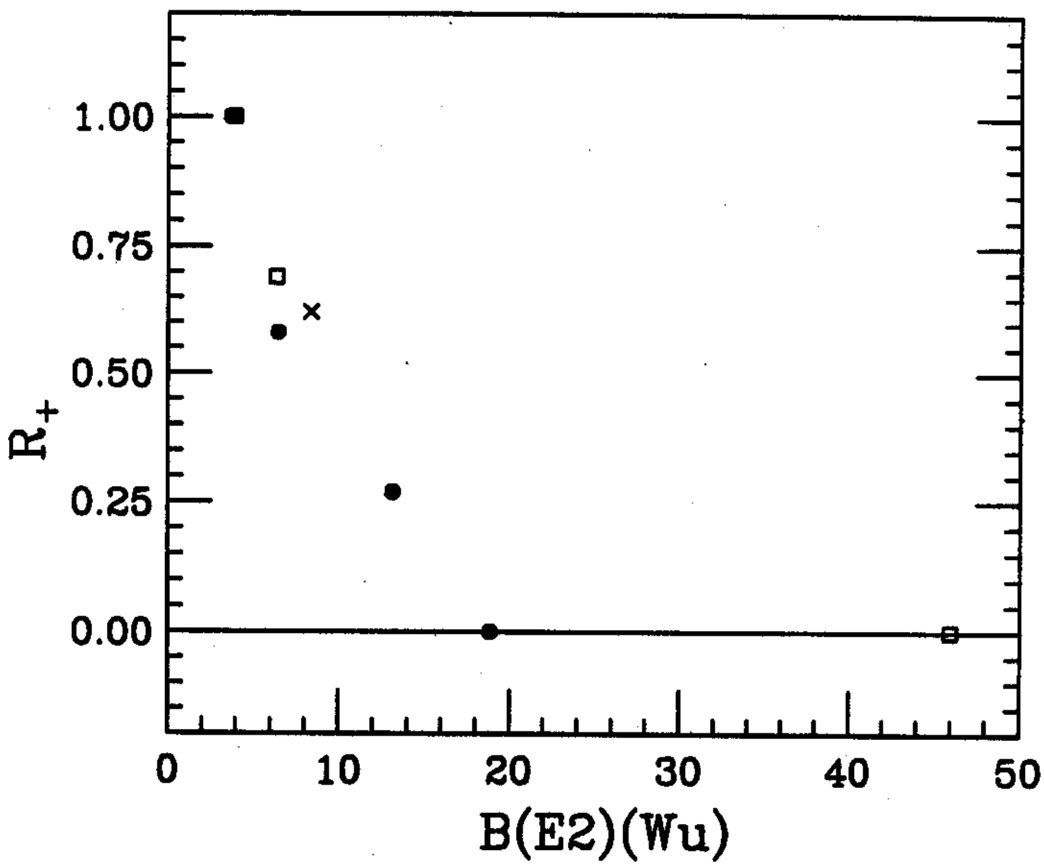

Fig. 4